Adaptation to Optimal Cell Growth through Self-Organized Criticality

Chikara Furusawa
Quantitative Biology Center, RIKEN, 6-2-3 Furuedai, Suita, Osaka 565-0874, Japan

Kunihiko Kaneko
Research Center for Complex Systems Biology, University of Tokyo, Komaba, Meguro-ku, Tokyo 153-8902, Japan
(Received 22 October 2011; published 15 May 2012)

A simple cell model consisting of a catalytic reaction network is studied to show that cellular states are self-organized in a critical state for achieving optimal growth; we consider the catalytic network dynamics over a wide range of environmental conditions, through the spontaneous regulation of nutrient transport into the cell. Furthermore, we find that the adaptability of cellular growth to reach a critical state depends only on the extent of environmental changes, while all chemical species in the cell exhibit correlated partial adaptation. These results are in remarkable agreement with the recent experimental observations of the present cells.

DOI: 10.1103/PhysRevLett.108.208103 PACS numbers: 87.17.Aa, 82.39.−k, 87.10.−e

Cells flexibly change their intracellular states with respect to environmental changes, so that they can sustain cellular growth under a variety of environmental conditions. Experimental analysis of microorganisms suggested that metabolic reactions can be organized to achieve optimal or nearly optimal growth under various environmental conditions [1]. Although environmental adaptation is generally explained by using signal transduction machineries as *lac* operon [2], it is difficult to imagine that such regulatory networks are prepared by evolution against unexpected environmental changes. Hence, it is natural to expect that cells will exhibit a rather generic, ubiquitous process of environmental adaptation, even in their primitive form. Given that all cellular processes are a result of complex chemical dynamics of catalytic reactions, to discuss the generic adaptation process of (primitive) cells, it is important to study how such a system with complex catalytic reaction networks can adapt to environmental changes and maintain optimal or nearly optimal growth.

In this Letter, we show that a simple active transport of nutrients enables generic adaptation toward a state with optimal growth, by simulating a simple cell model with a catalytic reaction network [3]. In our previous study [4], we showed that recursive cellular reproduction with optimal growth is achieved by controlling the flow rate of the nutrients, and we found that such optimal growth is achieved at a ''critical'' cellular state, in which the rank distribution of chemical abundance obeys a power law with exponent -1 (i.e., Zipf's law). Here, by introducing a simple active transport of nutrients, we show that the cellular dynamics are able to sustain optimal cellular growth by self-organization into a critical state [5].

In this study, we adopt a simple model of a reproducing cell with intracellular catalytic reaction networks that transform nutrient chemicals into other chemical species that exhibit catalytic activity [4,6]. Let us consider a cell consisting of N chemical species. The state of this cell can be represented by a set of chemical concentrations $(x_0, x_1, \ldots, x_{N-1})$, where x_i is the intracellular concentration of chemical species i. Depending on whether an enzymatic reaction occurs from i to j, catalyzed by some other chemical ℓ, the reaction path is connected as $(i + \ell \rightarrow j + \ell)$. The rate of increase in x_j and decrease in x_i through this reaction is given by $x_i x_\ell$. For the sake of simplicity, all the reaction coefficients have been set to 1. The connection paths of this catalytic network have been chosen randomly, where for all combinations of substrate i and product j the reaction path is randomly connected with a fixed probability ρ.

Next, some chemicals are supplied from the environment as nutrients. The transport of the chemical nutrients into the cell is activated with the aid of some other chemicals, i.e., ''transporters.'' Here, the uptake flux of the ith chemical from the environment is assumed to be represented by $F_i = S{x_{w_i}}^\alpha$, where the w_ith chemical acts as the transporter for chemical i and x_{w_i} is the concentration of the w_ith chemical. Parameter S denotes the concentration of the nutrient chemicals outside the cell and is a transport constant. Parameter α represents the higher-order effect in the nutrient transportation. If this parameter is greater than 1, the transporter catalysis is of a higher order, which corresponds to the formation of multimeric complex of the transporter. It should be noted that the cell volume increases with the abundance of chemicals within the cell. For the sake of simplicity, we assume that the cell volume is directly proportional to the total abundance of chemicals in the cell. The concentration of each chemical species is diluted with an increase in the cell volume by the nutrient transport. This assumption corresponds to imposing restriction $\sum_{i=0}^{N-1} x_i = \text{const}$, which can be set to 1 by appropriately normalizing the concentration variables.

To summarize these processes, the dynamics of the intracellular concentration of the ith chemical, where i is in the range $i = 0, 1, \ldots, N-1$, are represented as

$$\frac{dx_i}{dt} = \sum_{j,\ell=0}^{N-1} W_{ji\ell} x_j x_\ell - \sum_{j',\ell'=0}^{N-1} W_{ij'\ell'} x_i x_{\ell'} - x_i \sum_{j=0}^{N-1} F_j(+F_i), \quad (1)$$

where $W_{ij\ell}$ is 1 if reaction $i + \ell \rightarrow j + \ell$ occurs; otherwise, it is 0. The third term with the sum of nutrient uptake flux gives the constraint of $\sum_{i=0}^{N-1} x_i = 1$ because of the volume growth. The last term is added only for the nutrients, and it represents their transportation into a cell from the environment. For simplification purposes, we consider a cell with only one nutrient chemical and a corresponding transporter, whose concentrations are x_0 and x_1, respectively. Here, the cell growth rate is equal to the (total) nutrient uptake $F_0 = S x_1^\alpha$. We also assume that the nutrient chemical does not exhibit catalytic activity and cannot be the transporter.

Before describing the results of the present model, we note that, in the earlier model that did not include a transporter as in the case when $\alpha = 0$, we found that the transition occurred at a certain critical value of S, beyond which the cell could no longer grow continuously [4]. When the nutrient uptake rate exceeds the critical value, chemical reactions that transform the nutrient into other chemical substances, including catalysts, cannot follow the nutrient uptake. In such a case, the reaction network sustaining "metabolism" becomes unstable, which in turn eventually ceases the cell growth. This finding indicates that the critical nutrient uptake rate corresponds to the maximal capacity of the reaction network to assimilate the nutrient for recursive reproduction. Results of our study indicate that, at the critical nutrient uptake rate, the chemical abundance distribution obeys a power law, which is maintained by a hierarchical organization of enzymatic reactions. Furthermore, it should be noted that a maximal growth rate is achieved at this critical nutrient uptake rate.

Here, we numerically study the present model with $\alpha \geq 1$ by considering a variety of randomly chosen networks. Figure 1 shows a plot of the nutrient uptake F_0 (that corresponds to the growth rate) at the steady state against parameter S for the cases with $\alpha = 2$. For most cases, the system reaches a unique fixed-point attractor (see Fig. S1 [7] for exceptional cases). As shown in this figure, the nutrient uptake F_0 with a low concentration ($S < 10^{-3}$) increases proportionally with S, indicating that the concentration of transporter x_1 is almost unchanged. In contrast, when the concentration of the nutrients in the environment is high ($S > 1$), the nutrient uptake is sustained at a certain level, irrespective of S. This result implies that the concentration of the transporter decreases with an increase in S, in proportion to $S^{-1/\alpha}$. On the other hand, x_0 increases with S, and it was numerically found that $x_1 \propto (1 - x_0)^\beta$, where β depends on each network wherein β ranges from 2 to 5 (see the inset in Fig. 1). It is important to note that, in this region, the nutrient uptake is almost identical to the optimal nutrient uptake achieved only at the critical nutrient uptake for $\alpha = 0$ (denoted by the dotted line). In other words, over a wide range of parameter S, the cellular dynamics including the transporter concentration are self-regulated to achieve the critical state with an optimal-growth rate. This self-regulation of the transporter concentration is always achieved for any network and for any value of $\alpha \geq 1$, as long as the environmental nutrient concentration is higher than some value (Fig. S1 [7]).

The phenomenon of self-regulation to achieve criticality is explained as follows. When S is increased and when the nutrient uptake exceeds the critical level for reproduction, the nutrient concentration in a cell is too large; therefore, there is no room for producing all other non-nutrient chemicals [4]. Hence, the concentration of the transporter also decreases, which in turn causes the nutrient uptake rate to decrease down to the critical value. Here, the nutrient uptake regulates both the flow of chemical reaction from the nutrient and the dilution of chemical concentration due to the cellular growth. By achieving a balance between the production and dilution of the chemicals by negative feedback through the transporter concentration, the adaptive dynamics toward a state with a nearly optimal growth are self-organized.

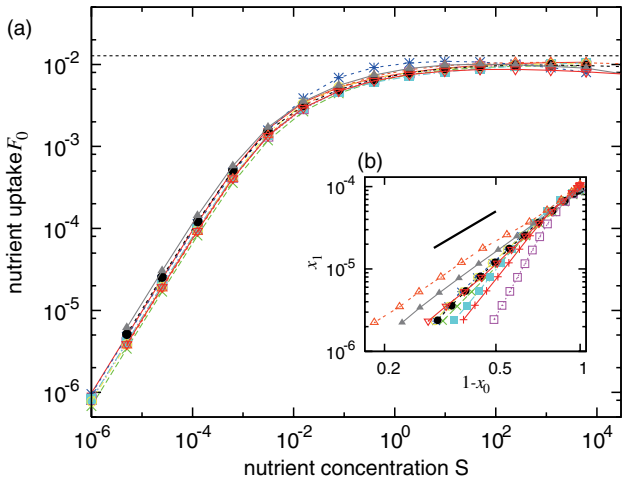

FIG. 1 (color online). Adaptive dynamics of nutrient uptake. (a) Nutrient uptake F_0 plotted as a function of the environmental nutrient concentration S. The results of ten randomly generated reaction networks are overlaid. The dotted line denotes the maximal nutrient uptake for the case $\alpha = 0$, beyond which the cell can no longer grow continuously. The parameters were set as $N = 10\,000$, $\rho = 2.5 \times 10^{-2}$, and $\alpha = 2$. (b) The concentration of transporter x_1 is plotted as a function of the total concentration of non-nutrient chemicals $1 - x_0$. The relationships obtained by ten random networks shown in (a) are presented. The solid line represents a slope of 2 for reference.

Figure 2 shows a plot of the rank-ordered distributions of the chemical concentrations obtained by a specific network for $\alpha = 2$, where the ordinate shows the chemical concentration x_i and the abscissa shows the rank determined by the magnitude of x_i. When the nutrient concentration S is low, the internal reaction dynamics progress faster than the flow of the nutrient from the environment, all the chemicals have nearly identical concentrations, and the influence of S is limited to a finite range of chemical species. For $S > 10$, where the nutrient uptake is close to the critical level, the distributions start to approximately follow a power law. Although the less abundant chemicals (e.g., rank >5000) exhibit some deviation, the exponent of the power law is close to -1 [8]. Indeed, such a power law was observed at the critical point with the maximal nutrient uptake in our previous study for $\alpha = 0$. This power law distribution with exponent -1 is attributed to the hierarchical organization of catalytic reactions, in which chemicals with low concentrations are produced from those with high concentrations [4]. In the present model, this power law holds as long as S is sufficiently high so that the nutrient uptake is self-regulated to a critical level. This confirms the self-organization of a cellular state to a critical state with optimal nutrient uptake.

This self-regulation to the critical state is also estimated by a simple "mean-field" calculation, by assuming the hierarchical flow of chemical reactions. Here, we consider a hierarchical layer of chemical species from the nutrient, as $L_0 \to L_1 \to L_2 \to \ldots L_k$, where L_0 denotes the nutrient chemical within the cell and L_i denotes a set of chemical species synthesized from L_{i-1} chemicals. We introduce m_i that denotes the mean concentration of L_i chemicals and assume that the concentrations of all enzymatic chemicals can be approximated by an identical mean-field value $(1 - m_0)/N$, the mean concentration of all non-nutrient chemicals [9]. Based on this mean-field approximation and by assuming that the transporter chemicals belong to the kth layer, we obtain

$$dm_0/dt = Sm_k^\alpha - (M/N)(1 - m_0)m_0 - Sm_k^\alpha m_0, \quad (2)$$

$$dm_j/dt = (M/N)[(1-m_0)m_{j-1} - (1-m_0)m_j] - Sm_k^\alpha m_j, \quad (3)$$

where $j = 1, \ldots, k$ and $M = \rho N$ denotes the mean number of reaction paths from each chemical. The last term in this equation represents the dilution of each chemical, attributed to the flow of nutrients. Then, we assume the steady state of chemical concentrations, i.e., $dm_j/dt = 0$ for $j = 0, 1, \ldots, k$. From $dm_0/dt = 0$, we obtain $F_0 = Sm_k^\alpha = (M/N)M_0 = \rho m_0$. By substituting it into Eq. (3) and assuming $dm_j/dt = 0$, we get $m_j = m_{j-1}(1-m_0)$. By iteratively applying this relationship, we get $m_k = m_0(1-m_0)^k$. From these equations, the steady values of F_0, m_k, and m_0 are obtained as functions of S. In particular, when S is large, $m_k \propto (1 - m_0)^k$ follows; this result is consistent with the numerical observation shown in Fig. 1(b) [10]. Furthermore, we obtain $F_0 \sim \rho$, indicating that the nutrient uptake F_0 is independent of the nutrient concentration when S is large. Indeed, this relationship $F_0 \sim \rho$ does not differ much from the numerical observation, as shown in Fig. 1. In the Supplemental Material [7], we provide an explanation for the power law distribution of chemical abundance with exponent -1, as shown in Fig. 2, by considering the conservation of chemicals and by using the above mean-field approximation.

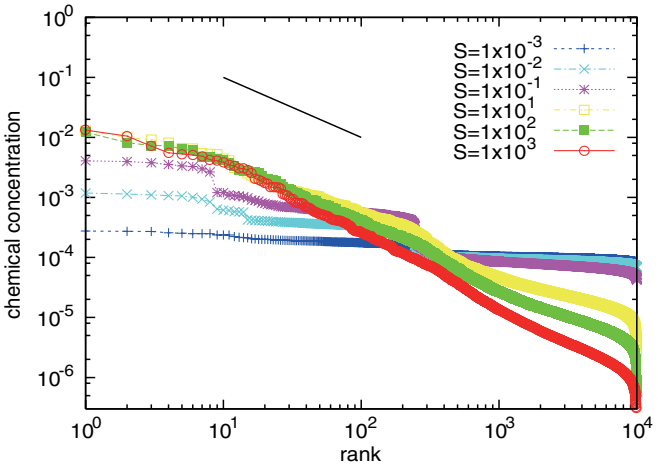

FIG. 2 (color online). Rank-ordered concentration distribution of chemical species. Distributions for different values of S are superimposed by using different colors. The solid line has a slope of -1 for reference. The other parameter values are identical to those shown in Fig. 1.

The self-regulation of the nutrient uptake rate to the critical value indicates that adaptive dynamics restore the nutrient uptake to the original level after environmental changes [11]. Figure 3 shows the adaptive dynamics of the nutrient uptake F_0 against the change in S from S_0 to S_0'. The response profile of F_0 to the environmental changes depends only on ratio S_0'/S_0. This type of adaptive response, termed fold-change detection, was recently confirmed in cellular responses [12]. Simple models of gene regulation or catalytic reaction involving few chemical components have been proposed to show such a type of adaptive dynamics [13,14]. In the present case, this fold-change detection is also shown from the mean-field equation in the large S limit. For example, let us consider the relaxation dynamics of Eqs. (2) and (3) with $k = 2$ toward the fixed point $[m_0 \approx 1 - (\rho/S)^{1/2\alpha}, \; m_2 \approx (\rho/S)^{1/\alpha}(1 - \rho/\alpha(\rho/S)^{1/2\alpha}]$. (Because $m_1 = 1 - m_0 - m_2$, there are only two independent variables.) For large S, the eigenvalues of the Jacobi matrix around the fixed point are given by $-\alpha\rho(1 \pm \sqrt{1 - 8/\alpha})/2$ and are independent of S. On the other hand, when S is changed from S_0 to S_0', the initial change in the nutrient uptake $F_0 = Sm_k^\alpha$ is solved from Eq. (1) to give $1/F_0(t) - (S_0/S_0')/F_0(0) =$

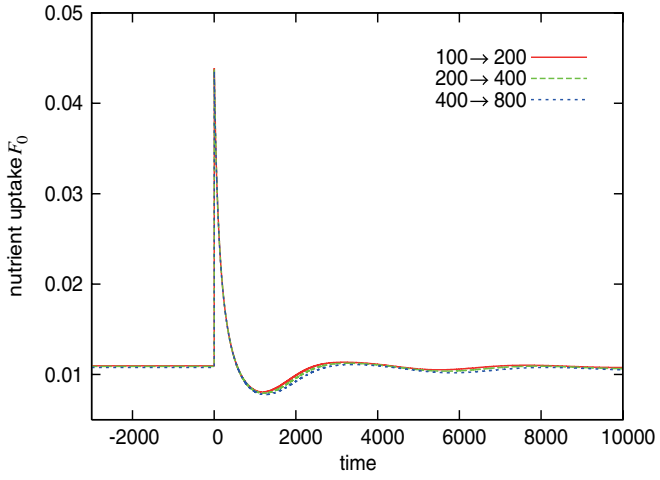

FIG. 3 (color online). Adaptation dynamics of the nutrient uptake F_0 after the environmental nutrient concentration S is changed. At $t = 0$, S is increased twice, and the responses corresponding to $S = 100 \rightarrow 200$, $S = 200 \rightarrow 400$, and $S = 400 \rightarrow 800$ are overlaid. The other parameter values are identical to those shown in Fig. 1.

$(1 - S_0/S_0')t$ (for small t and large S_0). Thus, the time course $F_0(t)$ depends only on the fold change S_0'/S_0; therefore, fold-change detection is demonstrated by using the mean-field approximation.

This perfect adaptation of the nutrient uptake (i.e., the cellular growth rate), as shown in Fig. 3, is supported by a large number of catalytic reactions through negative feedback control by a transporter. Besides the growth rate, the concentrations of all the chemical components (that are neither a nutrient nor a transporter) are changed to support the collective adaptive dynamics of the growth rate, against the change in S. It should be noted that, even though all the chemical components do not show perfect adaptation to return to the original value as in the case of the growth rate, in general, all the chemical components show partial adaptation [15], as shown in Fig. S2 [7]. It is interesting to note that such a partially adaptive response is observed for many gene expressions against environmental changes [16].

In conclusion, we have demonstrated that a cellular system consisting of a catalytic network shows optimal growth against environmental changes when nutrients are actively transported into the system with the help of a catalyst. It should be emphasized that the results reported herein are independent of the details of the modeling. They are also true for different kinetic forms in the catalytic reaction, different topologies of the reaction network such as the scale-free [17], and distributed reaction coefficients. For example, we confirmed that the use of Michaelis-Menten reaction kinetics with distributed coefficients does not change the present results, as long as a certain fraction of the reactions is in the linear regime. In fact, existing organisms would adopt sophisticated machineries in metabolic reactions, transcription, and translation. However, the self-organizing behavior for the adaptive growth regulation proposed herein emerges as long as the nutrient uptake dynamics are related to the intracellular dynamics and thus are expected to generally exist behind such sophisticated regulatory reaction processes. In fact, it is well known that the nutrient uptake in microorganisms is generally regulated by the intracellular reaction dynamics, such as a phosphotransferase system [18], which maintains a balance between the nutrient uptake and the metabolic activity. Furthermore, the synthetic activity of transporter proteins is also linked to the metabolic activity, and such processes generally include the higher-order effect as dimer and tetramer formation, proving that parameter $\alpha \geq 2$ in our model. Furthermore, it is interesting to note that this adaptation to optimal growth, power law in abundance distribution (Zipf's law), adaptive response with fold-change detection, and partial adaptation of many gene expressions are indeed generally observed in the present cells, supporting our hypothesis. We expect that the present self-organized criticality to the optimal-growth state will ubiquitously underlie the flexible and robust adaptation in cellular systems.

The authors thank T. Yomo, M. Inoue, Y. Kondo, and S. Ishihara for useful discussions. The present study is partially supported by the ERATO project, JST, and Grants-in-Aid for Scientific Research (No. 23680030, No. 23650152, and No. 21120004) from MEXT Japan.

[1] R. U. Ibarra, J. S. Edwards, and B. O. Palsson, Nature (London) **420**, 186 (2002); S. S. Fong and B. O. Palsson, Nat. Genet. **36**, 1056 (2004); Y. Shinfuku, N. Sorpitiporn, M. Sono, C. Furusawa, T. Hirasawa, and H. Shimizu, Microb. Cell Fact. **8**, 43 (2009).

[2] F. Jacob and J. Monod, J. Mol. Biol. **3**, 318 (1961).

[3] A. Filisetti, R. Serra, T. Carletti, M. Villani, and I. Poli, Eur. Phys. J. B **77**, 249 (2010); S. Jain and S. Krishna, Proc. Natl. Acad. Sci. U.S.A. **98**, 543 (2001); D. Segre, D. Ben-Eli, and D. Lancet, Proc. Natl. Acad. Sci. U.S.A. **97**, 4112 (2000).

[4] C. Furusawa and K. Kaneko, Phys. Rev. Lett. **90**, 088102 (2003).

[5] P. Bak, C. Tang, and K. Wiesenfeld, Phys. Rev. A **38**, 364 (1988); D. Dhar and R. Ramaswamy, Phys. Rev. Lett. **63**, 1659 (1989); H. J. Jensen, *Self-Organized Criticality: Emergent Complex Behavior in Physical and Biological Systems* (Cambridge University Press, Cambridge, England, 1998); A. Awazu and K. Kaneko, Phys. Rev. E **80**, 010902(R) (2009);

[6] C. Furusawa and K. Kaneko, Phys. Rev. E **73**, 011912 (2006); Y. Kondo and K. Kaneko, Phys. Rev. E **84**, 011927 (2011).

[7] See Supplemental Material at http://link.aps.org/supplemental/10.1103/PhysRevLett.108.208103 for Figs. S1 and S2 and supplemental text.

[8] The slopes in Fig. 2 obtained by the least squares fit are -1.04, -1.12, and -1.21 for $S = 10^1$, 10^2, and 10^3, respectively. For larger S, they might be slightly smaller

than -1, which is predicted by the mean-field approximation discussed later, presumably due to the finite size effect of the reaction network.

[9] Hence, the mean-field version differs from a one-dimensional chain of catalytic reactions, where adaptation to the critical state is not observed.

[10] In the simulations shown in Fig. 1, the transporter chemical is located at L_2 or L_3. The reason why the slopes in Fig. 1 (b) are sometimes greater than 3 is presumably because of the hierarchical structures of the catalysts, which are omitted in the mean-field calculation in Eqs. (2) and (3).

[11] D. E. Koshland, Jr., A. Goldbeter, and J. B. Stock, Science **217**, 220 (1982); F. Oosawa and Y. Nakaoka, J. Theor. Biol. **66**, 747 (1977); S. Asakura and H. Honda, J. Mol. Biol. **176**, 349 (1984); U. Alon, M. G. Surette, N. Barkai, and S. Leibler, Nature (London) **397**, 168 (1999).

[12] L. Goentoro and M. W. Kirschner, Mol. Cell **36**, 872 (2009); C. Cohen-Saidon, A. A. Cohen, A. Sigal, Y. Liron, and U. Alon, Mol. Cell **36**, 885 (2009); M. D. Lazova, T. Ahmed, D. Bellomo, R. Stocker, and T. S. Shimizu, Proc. Natl. Acad. Sci. U.S.A. **108**, 13 870 (2011).

[13] O. Shoval, L. Goentoro, Y. Hart, A. Mayo, E. Sontag, and U. Alon, Proc. Natl. Acad. Sci. U.S.A. **107**, 15995 (2010).

[14] M. Inoue and K. Kaneko, Phys. Rev. Lett. **107**, 048301 (2011)

[15] Adaptive dynamics of the cellular state is generally classified into ''perfect adaptation,'' in which a variable in concern returns to the original value after a response, and ''partial adaptation,'' in which the variable shows a change to decrease the response, but it does not return to the original value completely. See Koshland, Goldbeter, and Stock's paper in Ref. [11] for further details.

[16] A. P. Gasch, P. T. Spellman, C. M. Kao, O. Carmel-Harel, M. B. Eisen, G. Storz, D. Botstein, and P. O. Brown, Mol. Biol. Cell **11**, 4241 (2000); S. Stern, T. Dror, E. Stolovicki, N. Brenner, and E. Braun, Mol. Syst. Biol. **3**, 106 (2007).

[17] When the transporter is directly produced from the nutrient, feedback to the nutrient uptake often leads to oscillatory behavior, even in the case when $\alpha \geq 2$. However, as long as the transporter is not directly produced from the nutrient, the adaptive dynamics described here, as well as the power law in abundances, generally appears regardless of the position of the transporter in the reaction network.

[18] J. Deutscher, C. Francke, and P. W. Postma, Microbiol. Mol. Biol. Rev. **70**, 939 (2006).

Supplementary Text: A sketch of an explanation on Zipf's law from the mean-field analysis

The origin of power-law in abundances is due to hierarchical organization of abundances of chemicals. Although complete explanation on the organization of power-law is out of the scope of the simple "mean-field" calculation, here we provide a sketch for the explanation.

From the mean-field analysis in the text, we get that the mean concentration of a chemical at k-th layer obeys $m_k = m_0(1-m_0)^k$. On the other hand, at each k-th layer, there are $\sim (\rho N)^k$ chemical species. Hence, the ranking of the chemical at k-th layer, denoted by r_k, in the order of abundances increases as $r_k \sim (\rho N)^k$ when ρN is enough large, and thus $k = \log(r_k)/\log(\rho N)$. From these equations, we obtain $m(r_k) = m_0(1-m_0)^{\log(r_k)/\log(\rho N)}$, where $m(r_k)$ represents the chemical concentration of r_k-th ranked chemical. Thus,

$$\log m_k = \log m_0 - \alpha \log(r_k) \tag{S1}$$

with $\alpha = -\log(1-m_0)/\log(\rho N)$, so that the abundances against the ranking follows a power law with the exponent α.

Note that the total abundances of chemicals at each layer is roughly given by $m_0 C^K$ with $C = (1-m_0)(\rho N)$. The total sum of the abundances up to the maximal layer K should be $1-m_0$, so that

$$m_0 C \frac{(C^K - 1)}{C-1} \sim (1-m_0). \tag{S2}$$

Now, if $C > 1$, the left hand side of eq.(S2) diverges as K increases, and eq.(S2) cannot be satisfied. On the other hand, if $C < 1$, eq.(S2) in the large K limit would imply $m_0 C/(1-C) = 1-m_0$, which could be satisfied only if $\rho N = 1$, i.e., no branching at all between layers. Thus, for the self-consistency condition to satisfy eq.(S2) for the multiple branching case (i.e., $\rho N > 1$), $C = (1-m_0)\rho N \sim 1$ would be demanded, so that $\alpha \sim 1$. Hence the Zipf's law follows. Basically it is a result of the hierarchical organization of chemical reaction and the conservation law. Here, we note that this is a "self-consistency" argument, and whether the hierarchical organization in the mean-field approximation is unique in the original equation is not answered.

This approximation would be oversimplified, since in reality, the concentration of each chemical in a given layer is not identical, but differs by each element, depending on the abundances of the chemical that catalyzes its synthesis. Then, we need to take the hierarchical

organization not only as the substrate but also as the catalyst into account. Although this is beyond simple mean-field approximation, it might be expected that the above power-law abundances is also preserved within each layer, as the abundance of the catalyst follows the power law according to the above argument. Thus, Zipf's law across all chemicals is expected, even though complete derivation for it would possibly require advanced technique such as renormalization group.

Supplementary Figures

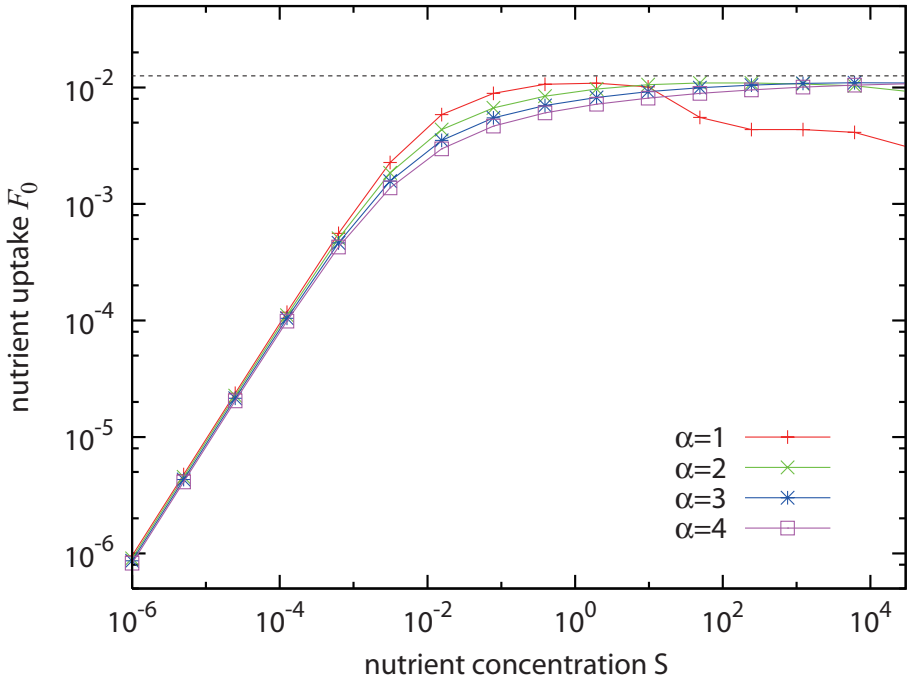

Fig. S 1: Adaptive dynamics of the nutrient uptake under different values of parameter α. This parameter α represents the higher order effect in the nutrient transportation, which is introduced to investigate the effect of the strength of negative feedback on the adaptive behavior. In the figure, scaled nutrient uptake $F_0 = S(Nx_1)^\alpha$ is plotted for easy comparison of results with different α. As shown in the figure, when $\alpha \geq 2$, the nutrient uptake F_0 is maintained close to the critical value, denoted by the dotted line, for wide ranges of the environmental nutrient concentration S. When $\alpha = 1$, the nutrient uptake decreases for most networks as S increases to a considerably high level, where the attractor ceases to be a fixed-point attractor. The concentrations of chemicals exhibit periodic or chaotic oscillation, which reduces the (average) nutrient uptake from the optimal value. This result suggested that the introducing a higher order effect increases the parameter range within which the self-regulation to the optimal growth is achieved.

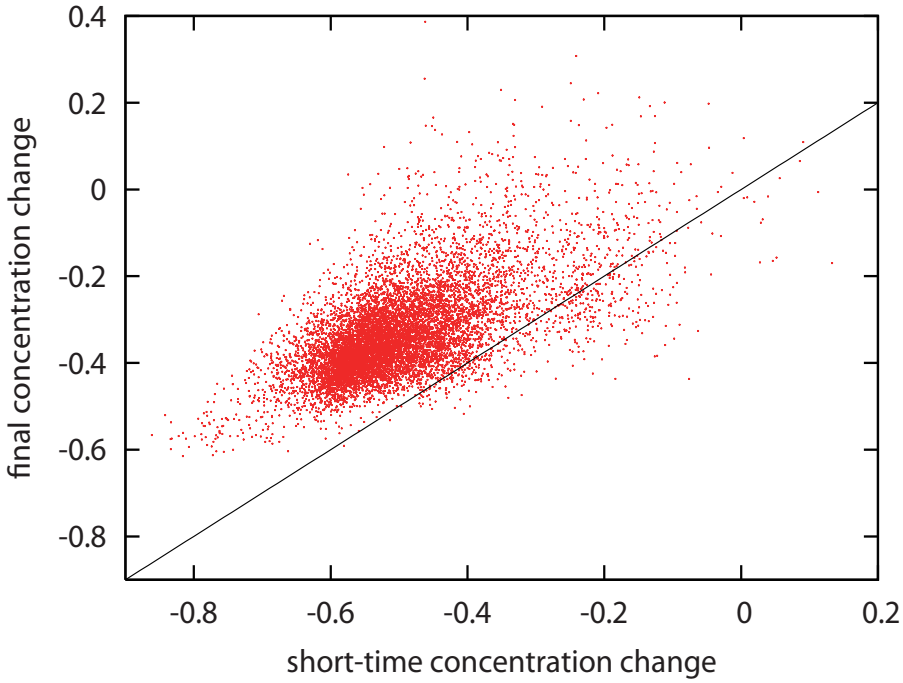

Fig. S 2: Relationship between the short-term response and the final concentration change after the environmental nutrient concentration S is changed. The other parameter values are identical to those used in Fig.1. The short-term response is obtained as the concentration ratio of chemicals between before ($t < 0$) and soon after changing S as $S = 100 \to 200$ ($t = 1500$ in Fig. 3). The final concentration change is calculated as the ratio between before changing S and after the dynamics stabilize to a fixed-point in the new environment. The $\log_{10}$-transformed concentration ratios are plotted. The solid line has a slope of 1 for reference. Recall that if perfect adaptation occurs, the points lie on the horizontal axis, whereas if adaptation does not occur, the points lie on the reference line with a slope of 1. Here, the points lie between these two lines, implying partial adaptation; these points are fitted around a slope of 0.66, suggesting that all chemicals show a common trend in partial adaptation.